NASA TECHNICAL REPORT

NASA TR R-439

4.

THERMAL LOADING IN THE LASER HOLOGRAPHY NONDESTRUCTIVE TESTING OF A COMPOSITE STRUCTURE

H. K. Liu and R. L. Kurtz

George C. Marshall Space Flight Center
Marshall Space Flight Center, Ala. 35812

3.

NATIONAL AERONAUTICS AND SPACE ADMINISTRATION • WASHINGTON, D. C. • MAY 1975

5.

1. REPORT NO.	2. GOVERNMENT ACCESSION NO.	3. RECIPIENT'S CATALOG NO.
NASA TR R-439		

4. TITLE AND SUBTITLE

Thermal Loading in the Laser Holography Nondestructive Testing of a Composite Structure

5. REPORT DATE
May 1975

6. PERFORMING ORGANIZATION CODE

7. AUTHOR(S)
H. K. Liu* and R. L. Kurtz

8. PERFORMING ORGANIZATION REPORT #
M133

9. PERFORMING ORGANIZATION NAME AND ADDRESS

George C. Marshall Space Flight Center
Marshall Space Flight Center, Alabama 35812

10. WORK UNIT NO.

11. CONTRACT OR GRANT NO.

13. TYPE OF REPORT & PERIOD COVERED

Technical Report

12. SPONSORING AGENCY NAME AND ADDRESS

National Aeronautics and Space Administration
Washington, D.C. 20546

14. SPONSORING AGENCY CODE

15. SUPPLEMENTARY NOTES

Prepared by Space Sciences Laboratory, Science and Engineering
*Associate Professor, University of Alabama Tuscaloosa and ASEE Fellow to MSFC

16. ABSTRACT

A unique laser holographic interferometry method that has variable sensitivity to surface deformation has been applied to the investigation of composite test samples under thermal loading. These experimental results are presented along with the mathematical analysis of the physical model of the thermal loading and current conduction in the composite material.

17. KEY WORDS

18. DISTRIBUTION STATEMENT

Unclassified – Unlimited

Cat 39

19. SECURITY CLASSIF. (of this report)	20. SECURITY CLASSIF. (of this page)	21. NO. OF PAGES	22. PRICE
Unclassified	Unclassified	23	$3.25

ACKNOWLEDGMENT

The authors appreciate the assistance of Mr. George Loughead in designing the loading plate, Mr. Dan Nisen in designing and building the heater, and Mr. Ken Savitz in taking the holograms, all of the Space Sciences Laboratory of the Marshall Space Flight Center.

TABLE OF CONTENTS

LIST OF ILLUSTRATIONS

THERMAL LOADING IN THE LASER HOLOGRAPHY NONDESTRUCTIVE TESTING OF A COMPOSITE STRUCTURE

I. INTRODUCTION

Holographic interferometry has been applied to the detection of bonding voids in rubber-to-metal, plastic-to-metal, and metal-to-metal laminates by the inspection of the deformation of the laminate surface [1] and the detection of defects of the bond between an inert solid fuel propellant grain and a polymer liner in the case of solid-fuel rocket motors [2]. Recently a unique laser holographic interferometry method with variable sensitivity has been successfully applied to the detection of tiny thin tapes (of thickness of 2.54×10^{-3} cm and an area of 1 mm^2) underneath a thick ceramic-epoxy-fiberglass composite plate [3] (of a thickness of 1.94 cm and an area of 232 cm^2). Planted debonds hidden inside the same plate have also been discovered in the same holographic nondestructive testing (HNDT) system while a pressure loading technique was applied.

All the aforementioned work has been based on the principle that stress-induced small surface deformation can be observed by the effect of constructive or destructive interference fringes either between the deformed object and the virtual image in the real-time case or the two virtual images displaced from each other in the case of double exposure. However, it is well known that, in general, two other object loading techniques are also available, namely, thermal loading and vibrational loading. In this report, the discussion shall be confined to thermal loading which offers an alternative means for the detection of debonds in the fiberglass-epoxy-ceramic radome structure.

An earlier report indicated that the results of the application of thermal loading to the detection of debonds in metal-to-metal structures were not encouraging [4]. Anomalous temperature-sensitive holographic fringe behavior was observed when such a loading was applied in the nondestructive testing of certain carbon-fiber reinforced plastics-skinned honeycomb structures [5]. None of these papers has presented a theoretical analysis of the thermal loading system that was applied.

The purpose of this report is to discuss the variable sensitivity HNDT system, present a mathematical analysis of the physical model of the thermal loading of the composite test samples, and provide a qualitative verification of the analytical results of the experimental observations.

The principles of the variable sensitivity laser holographic testing system are discussed in Section II. The test samples and the loading method are included in Section III. In Section IV, a simple model describing the thermal current conduction in the composite material is given. The experimental results are presented in Section V. Section VI provides the conclusions.

II. PRINCIPLES OF THE HNDT SYSTEM

To date holographic nondestructive testing has included many forms of wave interference phenomena. The following is a partial listing of some of the more useful and promising techniques:

1. Optical holography.
   a. Double-exposure techniques.
   b. Real-time technique.
   c. Vibration analyses technique.
   d. Correlation technique.

2. Acoustical holography.

3. Acousto-optical holography.

A summary of such techniques and descriptions of each may be found in References 6 and 7.

The first three optical holography techniques (a, b, and c above) are perhaps the most commonly applied techniques. Originally, however, each of these techniques required a specific arrangement of optical components, depending on what was to be tested and how it was to be loaded or stressed in order to locate a flaw or debond.

Recognizing that the sensitivity of the optical system employed is dependent on the direction of the light propagation vector with respect to the stress plane of the object, a new HNDT system which permits any form of loading (i.e., changes in subject amplitude as a result of loading) has been developed [8, 9]. This is accomplished by proper selection of geometry which allows minimum change in optical components to control the expected sensitivity [10].

This new system called a Composite Mobile Holographic Nondestructive Testing (CMHNDT) technique has variable sensitivity and, consequently, allows the three previously mentioned optical holography techniques to be combined into one hybrid type system. This hybrid system was used in the present thermal study and will now be briefly described. Using a variable sensitivity system, all three primary methods of HNDT can be accommodated with basically the same holographic arrangement (see Figure 1). Configuration No. 1 may be described as follows: Radiation emitted from the laser is incident on the field mirror assembly which contains a spatial filter and essentially a beam splitter. This assembly or unit is translatable to the left along the path ΔSb. The reflected portion of the radiation is made incident on the micrometer translatable object in such a direction as to make an angle equal to 0 with the perpendicular bisector of this object. This radiation is then turned antiparallel to itself where it passes on to the film recorder. The film recorder is itself translatable to the right along the path Δf.

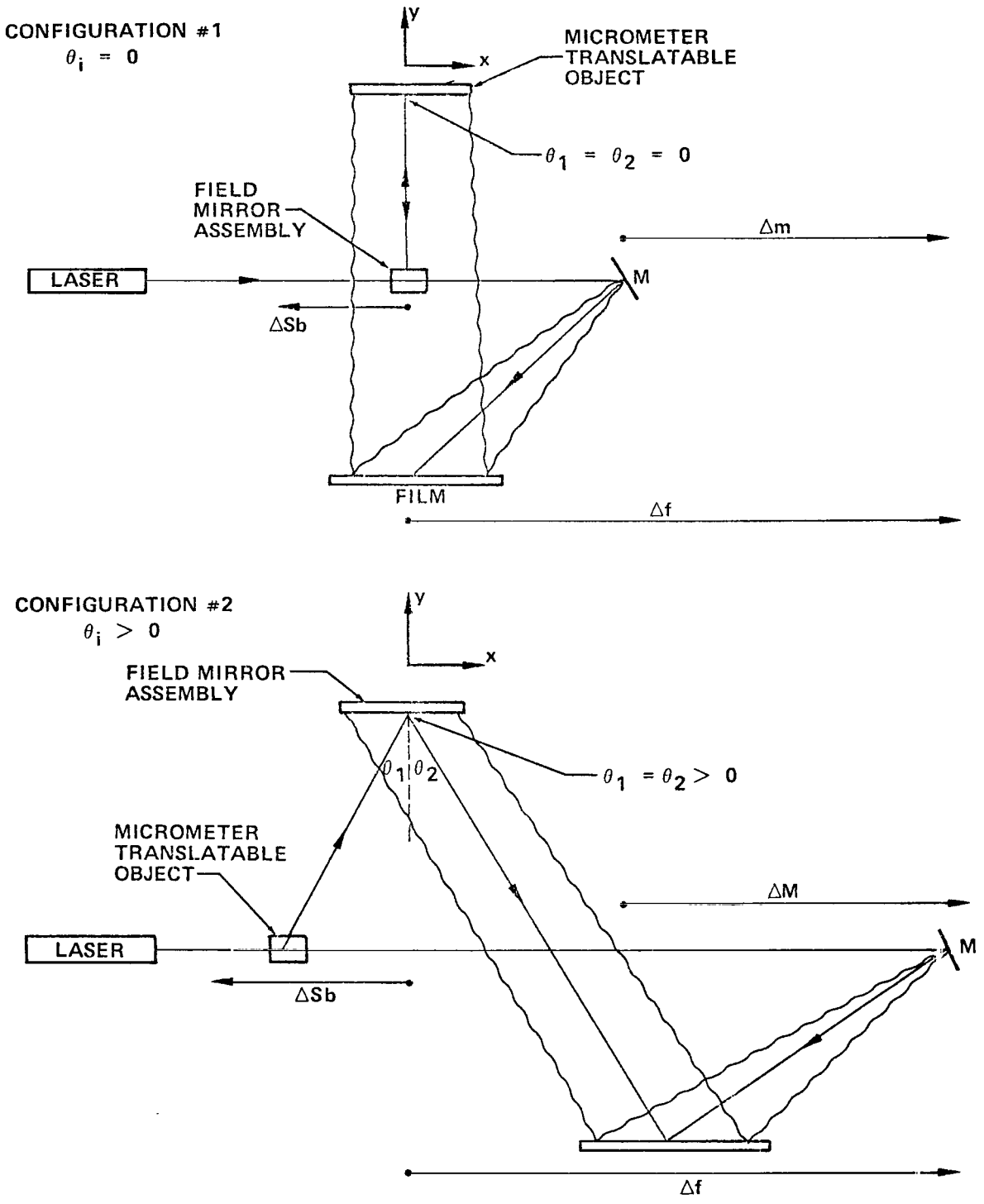

Figure 1. Composite Mobile Holographic Nondestructive Test System.

The radiation transmitted through the field mirror assembly is incident on mirror M, which is itself translatable to the right along path Δm. From here it is turned to be incident on the film recorder and interferes with the object beam.

Configuration No. 2 may be traced in a similar fashion, except that the object beam makes some angle $\theta > 0$ with the perpendicular bisector of the object.

The system is composite because one needs to only slightly manipulate three components (field mirror assembly, mirror M, and film recorder) to change from one method of HNDT to another. It is not necessary to establish a new geometry in order to perform the various HNDT methods. The system is mobile because all of the optical components are mounted on a precalibrated rigid table and may be locked in any position along their translatable paths. The system has variable sensitivity (which affords the composite structure) by virtue of the control over the angle θ which the object beam makes with the perpendicular bisector of the object.

Attention is directed to the equation of the double-exposure technique where the zeros indicating the presence of fringes occur for

$$m = \frac{2n-1}{2(\cos \theta_1 + \cos \theta_2)} \lambda \quad .$$

Consider the case of $\theta_1 = \theta_2 = 0$ deg, $\lambda = 5145$Å for an argon laser; then this equation becomes

$$m = (2n-1)\frac{\lambda}{4} = (2n-1)\frac{5145\ \text{Å}}{4} \quad ,$$

which says that the movement of the object (parallel or antiparallel to the k vector) of 0.1286 μm will be sufficient to cause one fringe to appear on the object.

On the other hand, consider the case of $\theta_1 = \theta_2 = 75$ deg and, again, $\lambda = 5145$Å; then this equation becomes

$$m = (2n-1)\frac{\lambda}{1.0353} = (2n-1)\frac{5145\text{Å}}{1.353} \quad ,$$

which says that, in order to obtain one fringe on the object, the movement of the object (in the same direction) must be as great as 0.4970 μm. While both of these movements are small, their relative values differ by about one-half order of magnitude. This provides an indication of the variation of sensitivity of this system by the minute adjustment of three single components on a precalibrated mobile table. The table is precalibrated in terms of the desired sensitivity.

Figure 2 is a schematic of this system as it was employed for this thermal study.

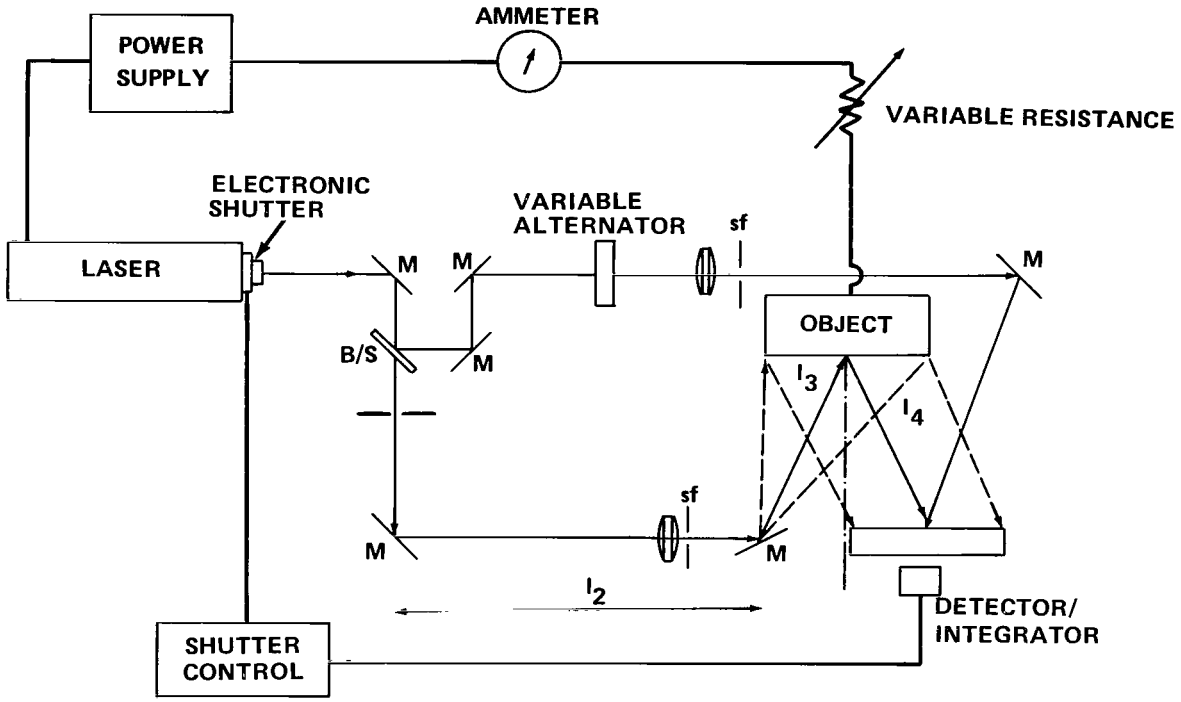

Figure 2. HNDT system diagram.

III. TEST SAMPLES AND THE THERMAL LOADING SYSTEM

A. Test Samples

The test samples were fiberglass-epoxy-ceramic sandwich structure as illustrated in Figure 3. Three kinds of flaws or debonds were programmed into the structure, as outlined by the dashed lines which represent the location projected on the 15.3 cm by 15.3 cm fiberglass surface. Three test samples of this type were provided. Common to these three samples, which are called test plates No. 1, No. 2, and No. 3, was an AF-32 plug precured all the way through the epoxy layers, as shown in the right-hand corner of

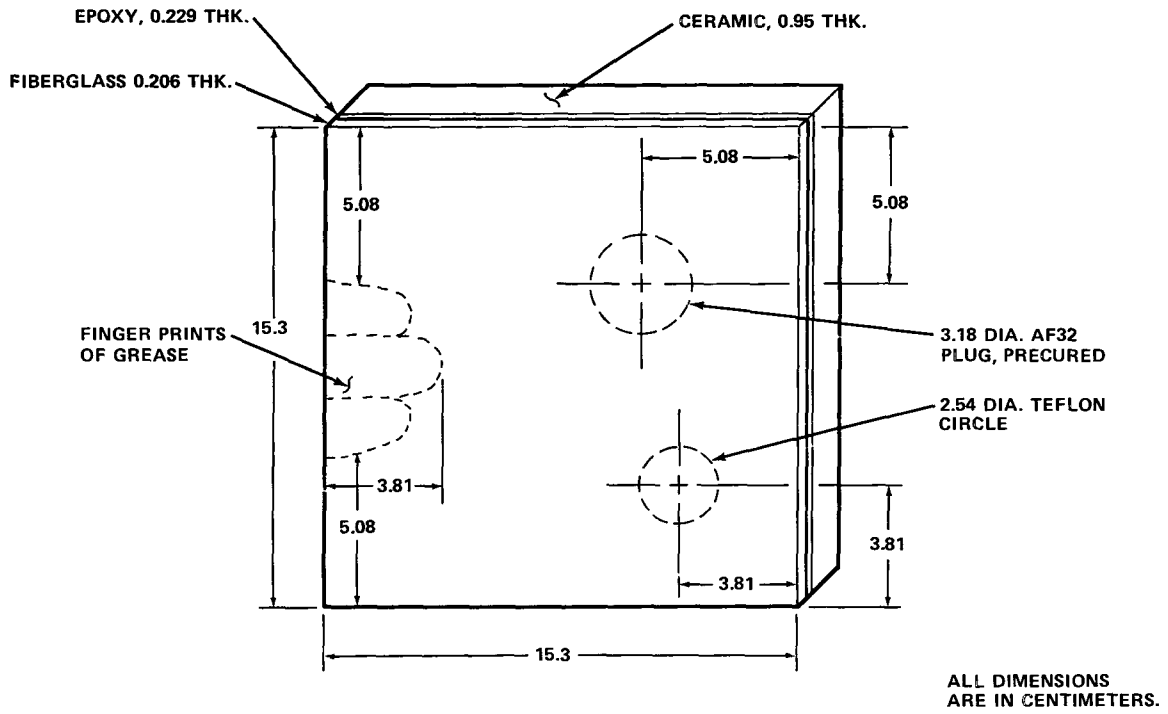

Figure 3. The structure of test samples.

Figure 3. Plates No. 1 and No. 2 had fingerprints of grease in the epoxy-ceramic interface, and the same type of fingerprints were put in the fiberglass-epoxy interface on plate No. 3. The vertical positions of the 2.54 cm diameter Teflon circles for the three samples were all different. The circle was on fiberglass for plate No. 1, on ceramic for plate No. 2, and in the middle of the four plies of epoxy for plate No. 3. These test plates are shown in Figure 4.

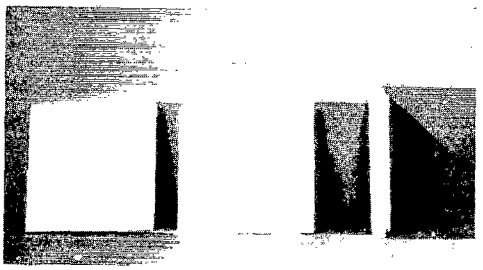

Figure 4. Test samples (l. to r., plate No. 1, No. 2, and No. 3).

B. Thermal Loading System

The design diagrams of the sample holder assembly and the heater connection are shown in Figure 5. The heater is connected through a variac to the ac source. The heater unit design is shown in Figure 6. The unit primarily consisted of a piece of 15 cm by 15 cm copper with an epoxy-glass laminate on its back and 0.02 cm stainless steel wire

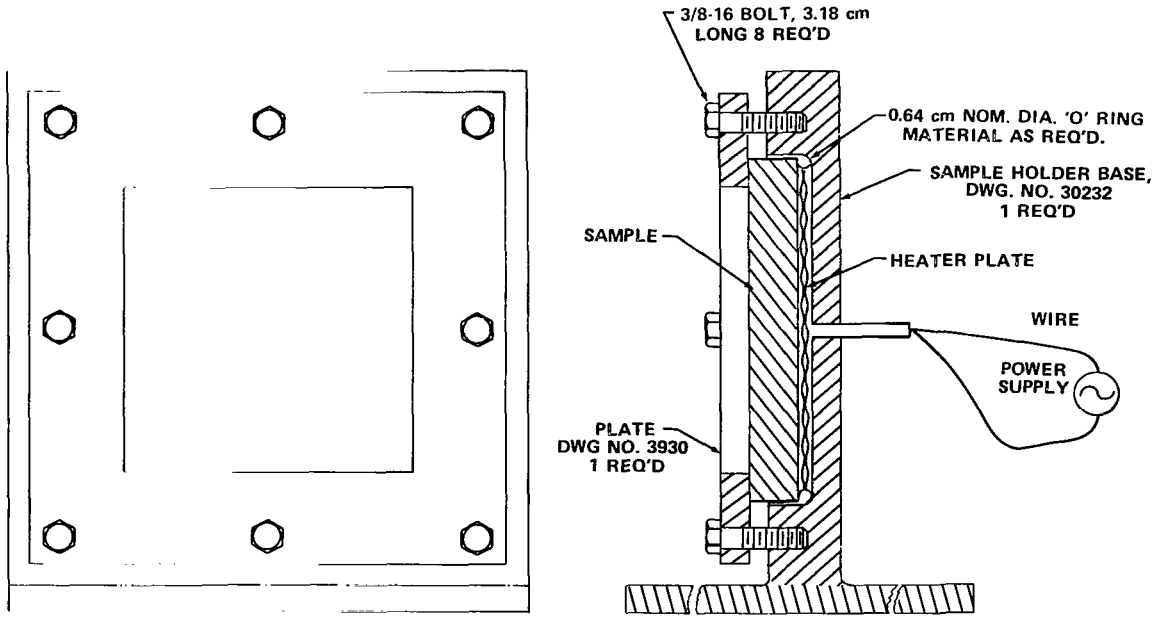

Figure 5. Design diagram of sample holder assembly and the heater plate connection in the thermal loading system.

wound on the glass surface. The wires are fastened to the glass surface by the glass epoxy. When current is passing through the wires and steady state is reached, uniform temperature on the front copper surface can be achieved.

The test sample holder and the overall view of the system are shown in Figure 7. In Figure 7a the variac is shown in the upper left corner, and its connection to the sample plate holder is shown in Figure 7b.

IV. THEORETICAL DISCUSSION OF THE THERMAL LOADING

Consider the cross section of the test plate as shown in Figure 8. The planted flaw is shown as the shaded region which has a front surface area A_2. The test plate has a front surface area A_1. The symbols T_x, T_y, T_z, and T_2, T_1 represent the temperature at the boundary surfaces and the two end surfaces, respectively, when steady state is achieved. The thickness of the various layers is expressed by L_1, L_2, L_x, and L_y. Thermal conductivities for the different layers are denoted by k_1, k_2, k_x, and k_y, respectively.

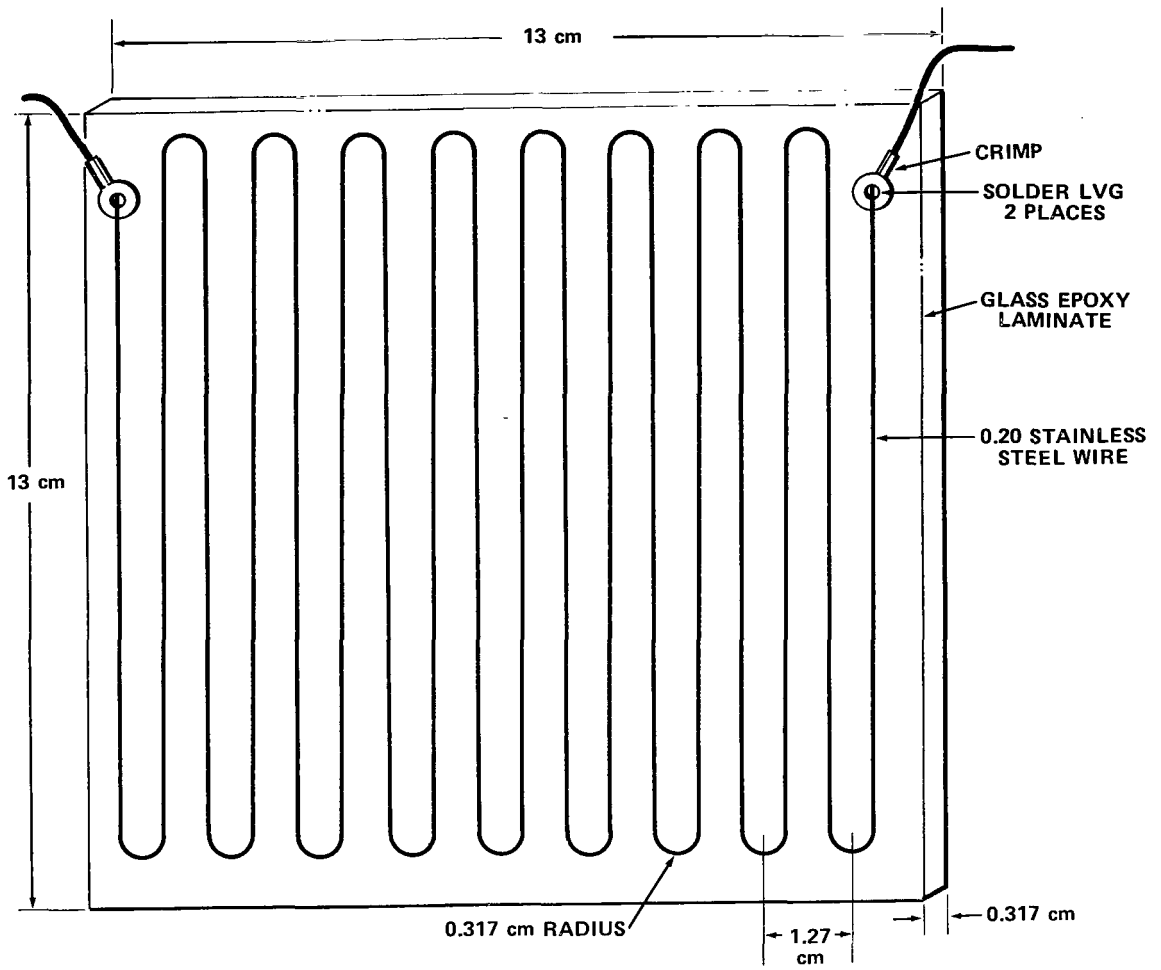

Figure 6. Design diagram of a glass laminate heater.

Assuming that (1) all the surfaces and interfaces have reached a uniform temperature as indicated in the figure, (2) lateral thermal current flow is negligible, and (3) $T_2 > T_1$, we may express the thermal current density j_1 through path 1 as follows

$$
\begin{aligned}
j_1 &= k_1 (T_z - T_1)/L_1 \\
&= k_y (T_y - T_z)/L_y \\
&= k_x (T_x - T_y)/L_x \\
&= k_2 (T_2 - T_x)/L_2
\end{aligned}
\tag{1}
$$

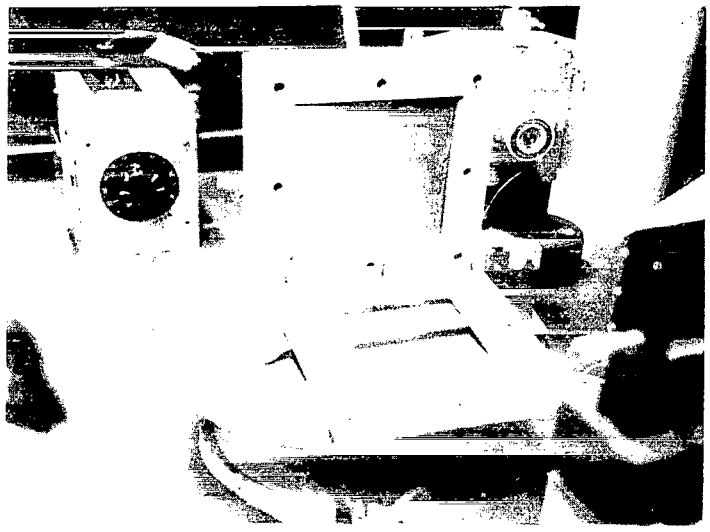

a. Sample holder.

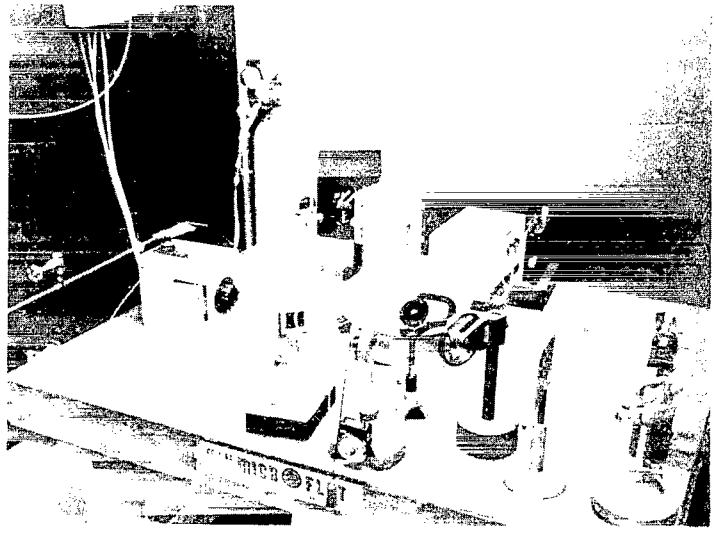

b. View of entire system.

Figure 7. Test sample holder and overall view of the system.

Notice that equation (1) in effect contains four equations, and the equivalence of these terms is based on the principle of current continuity. Solving equation (1) for j_1 by eliminating T_x, T_y, and T_z, we obtain

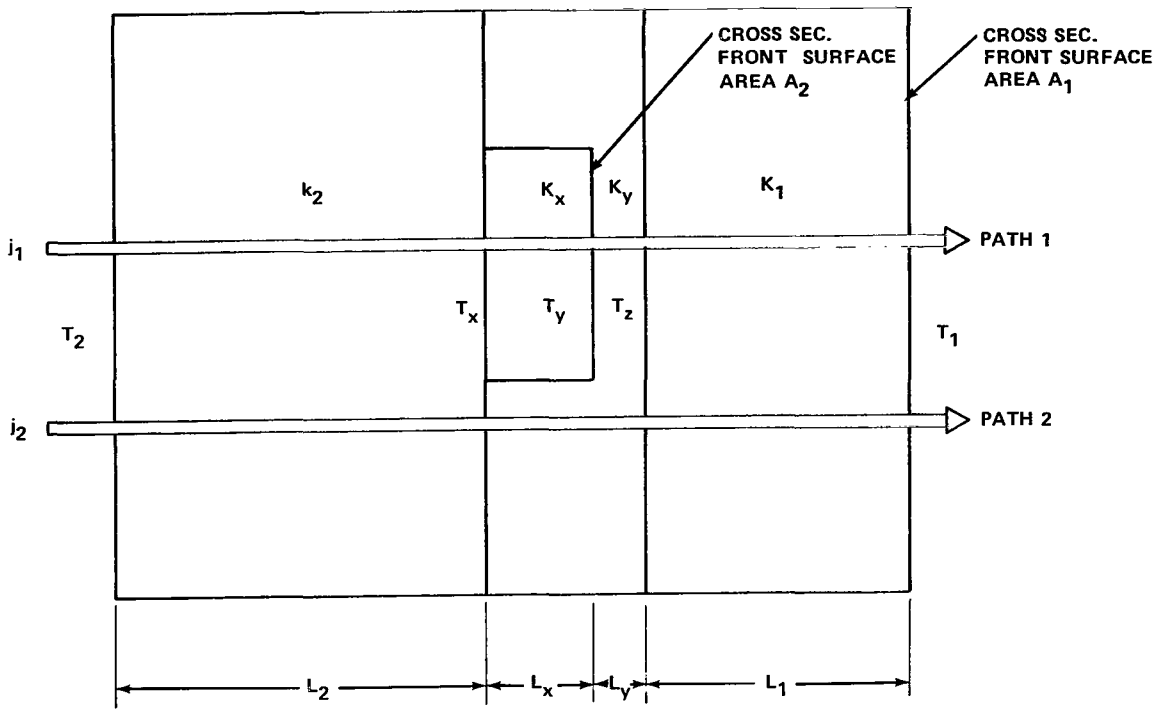

Figure 8. Cross section of the test plate.

$$j_1 = (T_2 - T_1)\,(L_1/k_1 + L_y/k_y + L_x/k_x + L_2/k_2) \quad . \tag{2}$$

This equation is a general expression for the steady-state thermal current density which is dependent on the material composition of the test plate. Similarly, thermal current density j_2 through path 2 may be expressed by

$$\begin{aligned} j_2 &= k_1\,(T_z - T_1)/L_1 \\ &= k_y\,(T_x - T_z)/(L_x + L_y) \\ &= k_2\,(T_2 - T_x)/L_2 \end{aligned} \tag{3}$$

Solving for j_2 from equation (3) by eliminating T_x and T_z, we obtain

$$j_2 = (T_2 - T_1)\,[L_1/k_1 + (L_x + L_y)/k_y + L_2/k_2] \tag{4}$$

It is important to see the difference between j_1 and j_2, since it is this difference which will cause the surface variations. After some arithmetic manipulations, percentage change of current density can be shown for the case $k_y > k_x$ as

$$\Delta j = 100 \times (j_2 - j_1)/j_2 = \frac{100\, L_x \left(\frac{1}{k_x} - \frac{1}{k_y}\right)}{\frac{L_1}{k_1} + \frac{L_x}{k_x} + \frac{L_y}{k_y} + \frac{L_2}{k_2}} \ (\%) \quad . \tag{5}$$

On the other hand, if $k_x > k_y$, then

$$\Delta j = 100 \times (j_1 - j_2)/j_1 = \frac{100\, L_x \left(\frac{1}{k_y} - \frac{1}{k_x}\right)}{\frac{L_1}{k_1} + \frac{L_x}{k_y} + \frac{L_y}{k_y} + \frac{L_2}{k_2}} \ (\%) \quad . \tag{6}$$

For example, if one considers k_2, k_x, k_y, and k_1 to be the thermal conductivities of the ceramic, Teflon, epoxy and fiberglass (S-glass), then their values are approximately 8.63×10^{-3} watt/cm-°K [11], 29.4×10^{-3} watt/cm-°K [12], 6.06×10^{-3} watt/cm-°K, and 20×10^{-3} watt/cm-°K [13], respectively. The lengths L_2, L_x, L_y, and L_1 for the composite plate in the present case are about 0.95 cm, 7.62×10^{-3} cm, 0.228 cm, and 0.206 cm, respectively. Since $k_x > k_y$, one substitutes these values into equation (6) and obtains the percentage variation of current densities as follows:

$$\frac{7.62 \times 10^{-3} \times \left(\frac{1}{6.06 \times 10^{-3}} - \frac{1}{29.4 \times 10^{-3}}\right) \times 100}{\left(\frac{0.206}{20 \times 10^{-3}} + \frac{7.62 \times 10^{-3}}{6.06 \times 10^{-3}} + \frac{0.228}{6.06 \times 10^{-3}} + \frac{0.95}{8.63 \times 10^{-3}}\right)} = 0.67\% \quad .$$

This difference of 0.67% in current densities Δj will cause different heat absorptions in the two corresponding regions. Consequently, the amount of surface variation due to the different thermal expansions in the Teflon washer region will be

different from the other surrounding regions. Laser holographic detection techniques should be sensitive enough to see this surface variation for sufficient temperature differences.

V. EXPERIMENTAL RESULTS

Before any of the test plates were put into the sample holder, a real-time hologram of the heater was taken and precisely replaced in the HNDT system. The purpose of doing this was to check the uniformity of the heat distribution over the copper surface of the heater. Smooth concentric circular fringe patterns were observed over the copper surface. With the addition of heat, the spacings between the fringes became smaller but the uniformity was preserved. This result indicated that the copper surface heated uniformly and that no flaw was shown in the heater.

When the test plate was placed into the sample holder, its surface temperature was monitored by a copper-constantan thermocouple. The position of the thermocouple was completely arbitrary; therefore, the temperature recorded should be considered as a kind of local temperature at the thermocouple's location. As we shall see, this temperature serves as a reference so that only its relative magnitude is of significance. The location of the temperature measurement was not critical in the present case.

The real-time interference fringe patterns with the fiberglass side (of the test plate) facing outward were recorded by a series of Polaroid pictures as the temperature was varied. Some of the pictures are shown in Figure 9. From this figure, one can see that the fringe patterns kept their uniformity, except at the edges, as the temperature was increased. However, the nonuniformities on those edges were primarily caused by the uneven stresses of the screws which were used to fix the test plates to the holder. Similar photographs were recorded when a real-time hologram for the ceramic side of test plate No. 1 was taken and replaced into the precision hologram holder. Photographs of these are shown in Figure 10. From the apparent uniformity of the fringes it is concluded that no flaw could be detected.

Following the same method, the fiberglass sides of plates No. 2 and No. 3 were investigated in the HNDT system. Photographs of the real-time interference fringe patterns are presented in Figures 11 and 12, respectively.

Figure 11 indicates that as the temperature on the fiberglass increased approximately 2°C, the flaws appeared in the form of nonuniformities of the fringes. These kinds of nonuniformities did not occur for plate No. 1 as shown in Figure 9. The edge effect also appeared as shown in the top center part in the picture. Figure 12 reveals phenomena similar to those in Figure 11. Therefore, from these two sets of pictures, the fringe patterns have disclosed all the three flaws programmed, as shown in Figure 3.

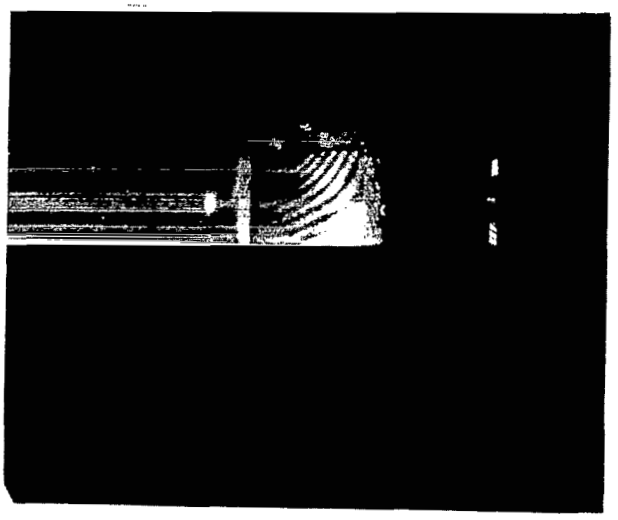

a. Real-time hologram taken at 21.25°C and replaced in hologram holder.

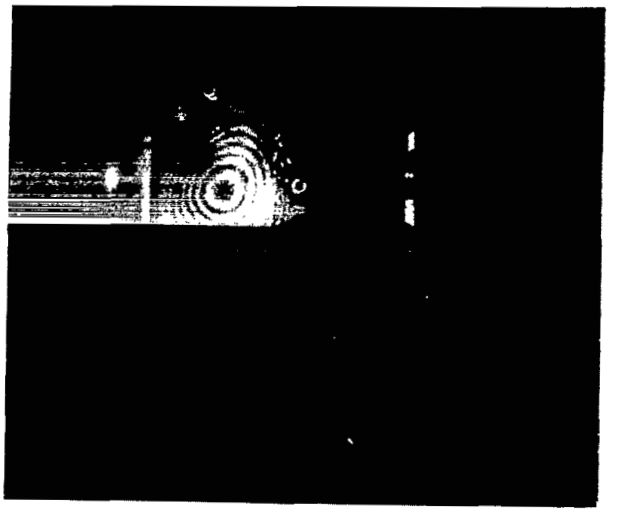

b. Same as (a) when T = 22°C.

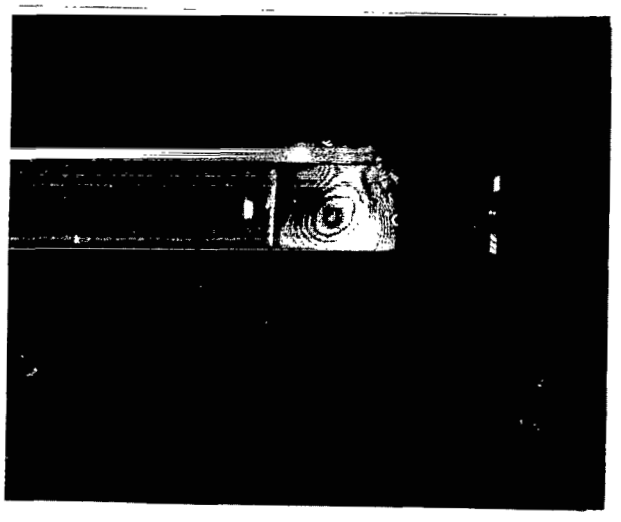

c. T = 23°C.

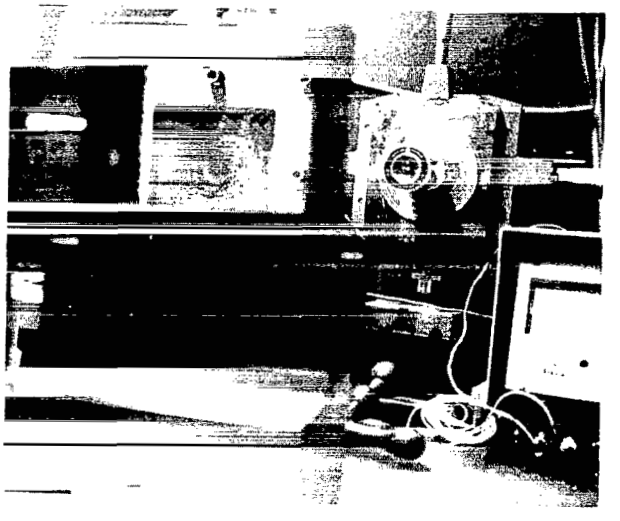

d. T = 24°C.

Figure 9. Real-time interference fringe pattern variations on the fiberglass surface of plate No. 1 as the temperature increased.

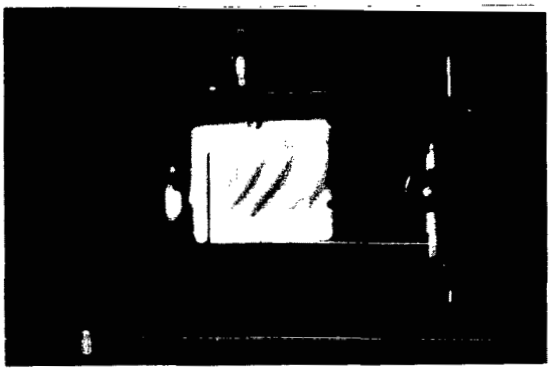

a. Real-time hologram taken at 19.2°C and replaced in the hologram holder. (Photograph taken at 19.25°C)

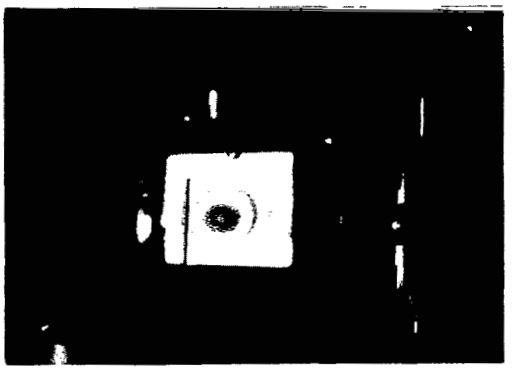

b. Same as (a) when T = 19.3°C.

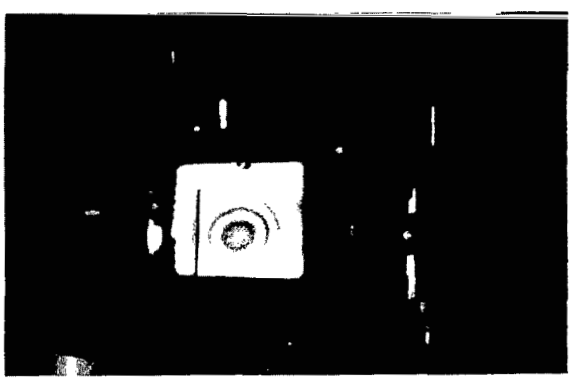

c. T = 19.35°C.

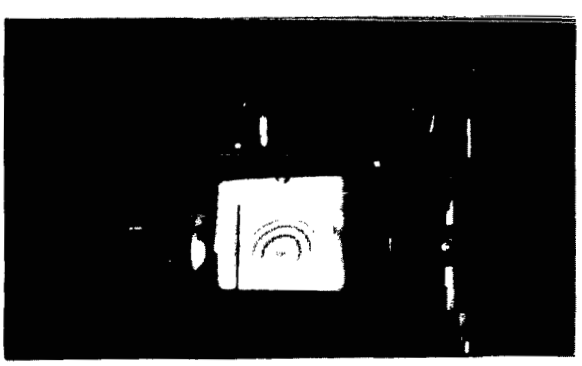

d. T = 19.4°C.

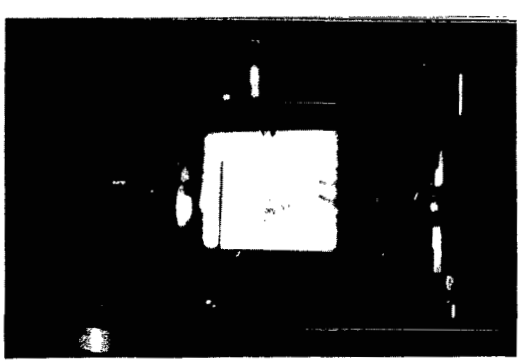

e. T = 20.25°C.

Figure 10. Real-time interference fringe pattern variations on the ceramic side of plate No. 1 as the temperature of the heater was increased.

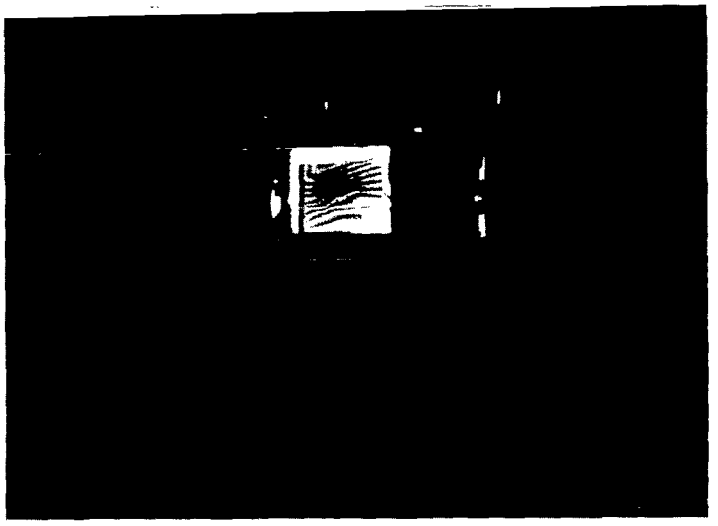

a. Real-time hologram taken at 18.4°C and replaced in the hologram holder. (Photograph was taken at T = 18.6°C).

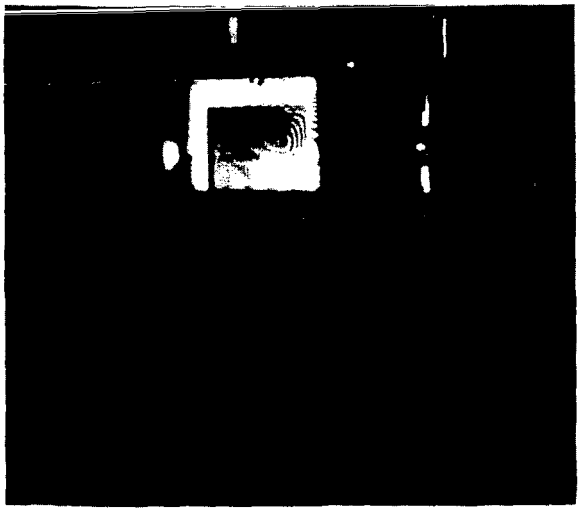

b. T = 20.5°C.

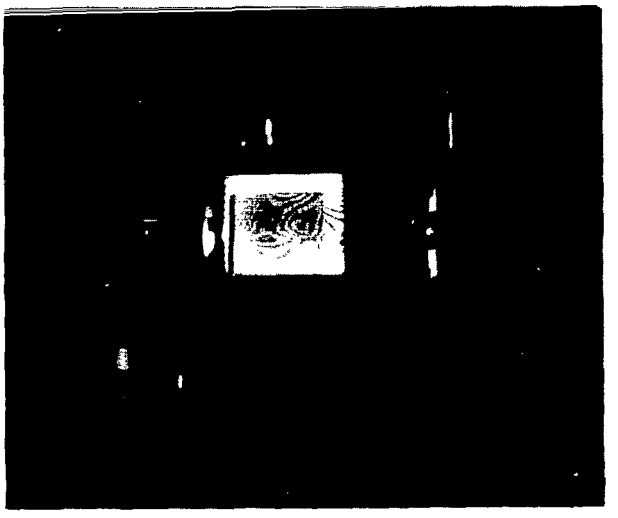

c. T = 20.6°C.

Figure 11. Real-time interference fringe pattern variations on the fiberglass side of plate No. 2.

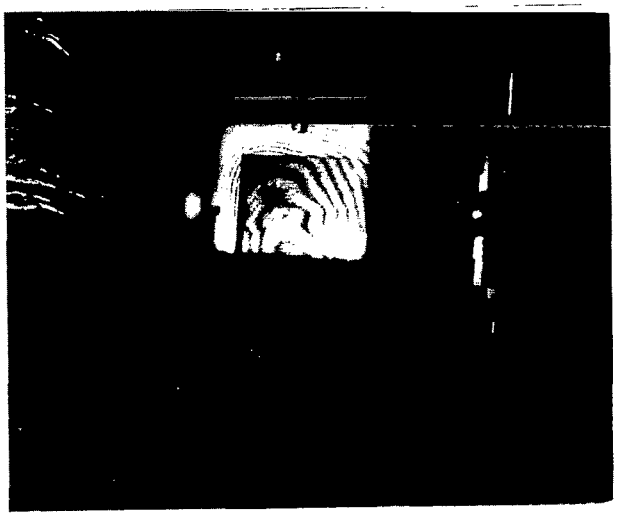

a. Real-time hologram taken at 19.8°C and replaced in the hologram holder. (Photograph was taken at T = 20°C).

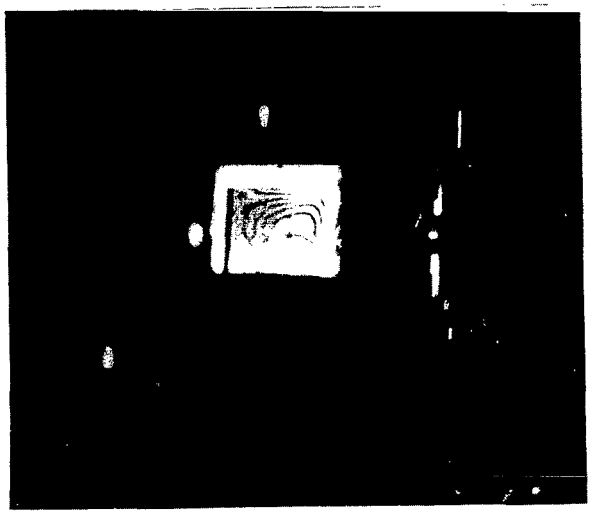

b. T = 21°C.

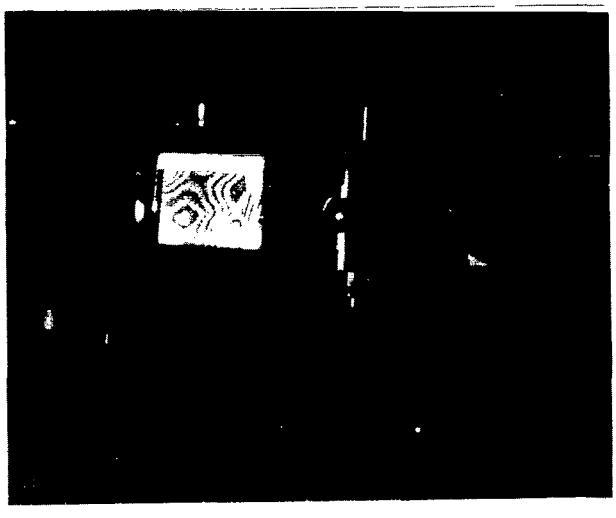

c. T = 21.3°C.

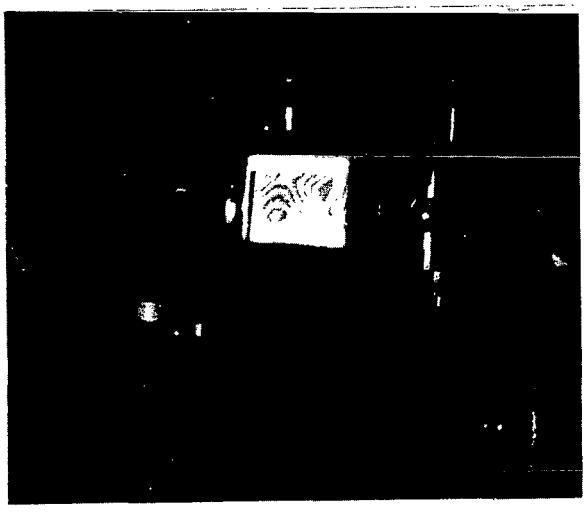

d. T = 21.5°C.

Figure 12. Real-time interference fringe pattern variations on the fiberglass side of plate No. 3.

It is interesting to note that the detection of these flaws could take place at a surface temperature lower than the room temperature and within a surface temperature variation of only a couple of degrees centigrade. The testing process is, therefore, considered to be highly sensitive and nondestructive for this kind of composite structure.

The theoretical model discussed in the last section may be applied to explain the results just obtained; i.e., differences in current densities cause differences in surface expansion which, in turn, affects the fringe pattern variations. The fact that plate No. 1 showed none of the programmed flaws was probably due to the fact that the debonds had rebonded again.

VI. CONCLUSIONS

It has been demonstrated by the experimental results that the present laser HNDT system incorporated with the thermal loading technique was sensitive enough to detect the preprogrammed hidden flaws from the fiberglass surface of the composite structure. A simple theoretical model for the thermal current density difference between flaw region and defect-free region has been formulated to explain the experimental results. The difference in thermal current densities indirectly revealed itself as interference pattern irregularities.

Assume that instead of the Teflon in the debond region there is an air gap of width (denoted by L_x as in Figure 8) 0.0762 mm. The thermal conductivity of air [13] at 18.2°C is 0.25×10^{-3} watts cm^{-1} $°K^{-1}$. The current density difference may be calculated if one substitutes the above value of thermal conductivity for k_x into equation (6) and keeps everything else the same. After the substitution and some computation, one obtains a current density difference of about 2.86 percent. The percentage is four times that in the case when the gap is filled with Teflon. Therefore, it may be concluded that reasonably small air gaps caused by epoxy debond should also be easily discovered by the thermal loading method.

In addition to the experimental results reported herein, the thermal loading technique was also applied to some thin Kapton cord material (of 2.54×10^{-3} cm thick), copper-clad printed circuit boards. Planted flaws, such as pieces of thin wires which were sandwiched between two boards, were also successfully detected. Since the testing temperatures were so low, the loading method offered at least a complementary means for the nondestructive testing of the composite structure.

George C. Marshall Space Flight Center
National Aeronautics and Space Administration
Marshall Space Flight Center, Alabama, September 1974
983-15-28-0000

REFERENCES

1. Iversen, R.J.; Mogarvery, J.W.; and Gardner, L.B., D.SC.: Holographic Inspection of Laminate Bonds. U.S. Army Weapons Command, Rock Island, Ill., Available from NTIS, 1970.

2. Waters, J.P.: Holographic Inspection of Solid Propellant to Linear Bonds. Appl. Opt., vol. 10, Oct. 1971. pp. 2364-2365.

3. Liu, H.K. and Kurtz, R.L.: Laser Holographic Detection on Tiny Thin Tapes Beneath a Thick Opaque Composite Structure. Proc. of 1974 IEEE Southeast Conference, April 30-May 1, 1974. Orlando, Fla.

4. Schliekelmann, R.S.: Non-destructive Testing of Adhesive Bonded Metal-to-Metal Joints, 2. Non-Destructive Testing, June 1972, pp. 144-153.

5. Marchant, M.: Temperature Sensitivity of CFRP Honey-comb Structures under Holographic NDT. Non-Destructive Testing, Feb. 1973. pp. 14-15.

6. Non Destructive Testing – A Survey. NASA SP-5113, 1973.

7. Holography – A Survey. NASA SP-5118, 1973.

8. Kurtz, R.L. and Liu, H.K.: Holographic Nondestructive Tests Performed on Composite Samples of Ceramic-Epoxy-Fiberglass Sandwich Structure. NASA TR R-430, June 1974.

9. Liu, H.K. and Kurtz, R.L.: Optical Holographic Nondestructive Testing of Composite Structure. University of Alabama BER Reports on ASEE-NASA Summer Faculty Fellowship Program, Aug. 1973.

10. Kurtz, Robert L.: A Holographic System for Nondestructive Testing – A Patent. MSFC Case No. 21704, Aug. 8, 1973.

11. Walton, J.D., Jr.: Radome Engineering Handbook. Marcel Dekker, Inc., New York, 1970, pp. 275-203.

12. Modern Plastics Encyclopedia, vol. 48/no. 10A, McGraw-Hill, 1971-1972.

13. Touloukian, Powell, Ho, and Klemens: Thermal Conductivity of Nonmetallic Solids. Thermophysical Properties of Matter, vol. 2, IFI/Plenum, 1970, pp. 922-923.

14. Thermal Conductivity of Nonmetallic Liquides and Gases. Thermophysical Properties of Matter, vol. 3, IFI/Plenum, 1970, p. 383.

NASA-Langley, 1975

"The aeronautical and space activities of the United States shall be conducted so as to contribute . . . to the expansion of human knowledge of phenomena in the atmosphere and space. The Administration shall provide for the widest practicable and appropriate dissemination of information concerning its activities and the results thereof."

—NATIONAL AERONAUTICS AND SPACE ACT OF 1958

NASA SCIENTIFIC AND TECHNICAL PUBLICATIONS

TECHNICAL REPORTS: Scientific and technical information considered important, complete, and a lasting contribution to existing knowledge.

TECHNICAL NOTES: Information less broad in scope but nevertheless of importance as a contribution to existing knowledge.

TECHNICAL MEMORANDUMS: Information receiving limited distribution because of preliminary data, security classification, or other reasons. Also includes conference proceedings with either limited or unlimited distribution.

CONTRACTOR REPORTS: Scientific and technical information generated under a NASA contract or grant and considered an important contribution to existing knowledge.

TECHNICAL TRANSLATIONS: Information published in a foreign language considered to merit NASA distribution in English.

SPECIAL PUBLICATIONS: Information derived from or of value to NASA activities. Publications include final reports of major projects, monographs, data compilations, handbooks, sourcebooks, and special bibliographies.

TECHNOLOGY UTILIZATION PUBLICATIONS: Information on technology used by NASA that may be of particular interest in commercial and other non-aerospace applications. Publications include Tech Briefs, Technology Utilization Reports and Technology Surveys.

Details on the availability of these publications may be obtained from:

SCIENTIFIC AND TECHNICAL INFORMATION OFFICE

NATIONAL AERONAUTICS AND SPACE ADMINISTRATION

Washington, D.C. 20546